Journal of Constructional Steel Research 153 (2019) 343–355

Contents lists available at ScienceDirect

Journal of Constructional Steel Research

# Influence of mechanical and geometric uncertainty on rack connection structural response

Federico Gusella [a,*], Sanjay Raja Arwade [b], Maurizio Orlando [a], Kara D. Peterman [b]

[a] University of Florence, Department of Civil and Environmental Engineering, Italy
[b] University of Massachusetts Amherst, Department of Civil and Environmental Engineering,USA

ARTICLE INFO

*Article history:*
Received 12 May 2018
Received in revised form 28 July 2018
Accepted 24 October 2018
Available online 3 November 2018

*Keywords:*
Rack connections
Sensitivity analysis
Monte Carlo simulation
Component Method
System reliability
Probabilistic assessment

ABSTRACT

Steel storage pallet racks are used worldwide for storage of palletized goods and are popular for their ease of construction, customization, and economy. Failure of these racks can result in significant property loss and economic disruption. Ultimately, the structural behaviour of these systems can be characterized as braced systems, in the cross-aisle direction, and un-braced moment resisting frame systems, in down-aisle direction. The structural capacity of these moment resisting frames depends on the performance of beam-to-column connections. Rack connections are typically formed by beams welded to connectors with tabs and columns with perforated cross-sections to accept these tabs joining beams and columns without bolts. This paper aims to evaluate the influence on the structural response of rack connection due to the structural details, and randomness in the geometrical features and mechanical properties of connection members (beam, weld, connector and column). To explore the impact of variability in design parameters on the initial flexural stiffness and ultimate flexural capacity of rack connections, a Monte Carlo simulation was conducted, using the Component Method to model the connection. Variability in member geometrical features was determined from current design specifications, while variability in steel mechanical properties was determined via experimental tests. The results indicate that system effects reduce flexural stiffness and the variability in the response of individual components does not propagate to the overall flexural capacity. Ultimately, the work motivates accurate and thorough reporting of geometric and structural uncertainty to accurately assess rack connection performance.


## 1. Introduction

Cold-formed steel (CFS) is commonly utilized in steel storage selective pallet racks that are popular in warehouses and other short- and long-term storage facilities [1]. Rack structures behave like bracing systems in the cross-aisle (transverse) direction, with uprights (columns) connected by diagonal bracing. In down-aisle (longitudinal) direction, bracing is rarely installed in order to make palletised goods readily accessible; therefore, racks behave like moment resisting frames (MRF) in which down-aisle stability and seismic resistance depend on the performance of beam-to-column connections [2–7].

Rack connections are composed of beams, typically a rectangular tubular cross-section welded to connectors with tabs, and cold-formed thin-walled steel columns, with arrays of holes along the length. These holes allow the beam to be connected at various heights without bolts for ease of assembly and adjustment [8].

These construction details result in complex numerical analysis difficult to translate to design recommendations [9]. Therefore, experimental tests methods have been necessary to evaluate the moment-rotation characteristics of rack connections for the current design codes [10–12]. Experimental testing has been particularly useful for determining seismic performance, providing useful information about the semi-rigid behavior and high ductility of these connections [13–18]. Despite the success and popularity of experimental testing, experimental tests can be expensive and time-consuming. Therefore current state-of-art models for steel joints are based on the Component Method (CM) whereby a joint is modelled theoretically as an assembly of components with an elasto-plastic or rigid force-displacement relationship [19]. Mechanical models based on the CM are able to evaluate the initial rotational (flexural) stiffness and ultimate moment of rack connections, both fundamental parameters in the design and analysis of rack structures under seismic loads [19]. Initial rotational stiffness is also critical for determining deflection limit states under service loads which typically govern rack beam design [20].

The moment-rotation characteristics of rack connections are influenced by several design parameters: structural properties of

* Corresponding author.
*E-mail addresses:* federico.gusella@unifi.it (F. Gusella), arwade@umass.edu (S.R. Arwade), maurizio.orlando@unifi.it (M. Orlando), kdpeterman@umass.edu (K.D. Peterman).

https://doi.org/10.1016/j.jcsr.2018.10.021
0143-974X/

connection members (beam, connector, beam-connector weld and column), steel material (mechanical) properties, and geometric manufacturing imperfections. This paper evaluates the propagation of uncertainty in component geometry and mechanical properties to the response of the complete connection in terms of initial elastic flexural stiffness and ultimate moment. A mechanical model based on the application of the CM, developed and validated in [21,22], through a comparison with experimental tests on full scale rack connections [16], has been adopted to conduct a Monte Carlo simulation of rack connections. These Monte Carlo simulations were then used to explore the variability of connection response to more accurately assess the structural performance of these joints.

In additional to the uncertainty quantification, a sensitivity analysis is performed to identify the quantities influencing joint structural response. With these findings, quality control efforts could be focused on promoting stability in statistical parameters to ensure reliability of rack joints [23,24]. Monte Carlo simulation of several models of steel rack connections is used to assess component vs. system sensitivity [25,26] and to evaluate the resultant variability in the value of initial rotational stiffness and ultimate flexural capacity from uncertainty in steel material properties and geometric manufacturing tolerances.

This paper begins with a presentation of the general characteristics of the rack. Using the CM, we present a detailed mechanical model of the connection, used to compute the initial rotational stiffness and ultimate flexural capacity. The same connection is then characterized via probabilistic models and random variables, and this characterization is implemented within the CM framework. The paper concludes with an analysis and discussion of the Monte Carlo simulations and with recommendations for designers.

## 2. Structural system and mechanical model

### 2.1. Structural scheme

In steel storage pallet racks, cold-formed steel (CFS) beams and uprights (columns) are connected through boltless joints, so beams can be easily disconnected to accommodate changes to the rack geometric layout. Rack connections are typically assembled with hollow tube beams welded to cold-formed angles with tabs (connectors) that are inserted into the slots of the columns. A sketch of a typical rack connection, with its members identified, is shown in Fig. 1.

In order to evaluate the moment-rotation characteristics of these rack connections and to assess the influence of different structural details on its mechanical behavior, a suite of full-scale connections were tested at the Structures and Material Testing Laboratory at the University of Florence. The test program involves varying the beam cross-section, weld between the beam and connector, connector type, and open mono-symmetric column cross-section [27,28] as summarized in Table 1.

**Table 1**
Parameters varied in experimental testing at the University of Florence.

| Member | Type | Geometric properties | | |
|---|---|---|---|---|
| | | Height [mm] | Width [mm] | Thickness [mm] |
| Beam | 1042 | 100 | 40 | 2 |
| | 1242 | 120 | 40 | 2 |
| | 1352 | 130 | 50 | 2 |
| Column | 70/150 | 68 | 72 | 1.5 |
| | 90/150 | 78 | 92 | 1.5 |
| | 110/200 | 84 | 112 | 2 |
| | 130/200 | 102 | 132 | 2 |
| | 130/250 | 102 | 132 | 2.5 |
| Connector | M4 (4 tabs) | 195 | 82 | 3.5 |
| | M5 (5 tabs) | 245 | 82 | 3.5 |
| Weld | A | Three-sided welding | | |
| | B | Double-sided welding | | |

Fig. 2 depicts the geometric properties of the rack connection members.

The as-tested experimental configurations are shown in Table 2. Numerical modeling was performed for all configurations.

### 2.2. Experimental tests

Moment-rotation curves for the rack connections were obtained through the test procedure proposed in [12]. A load $P$ (as shown in Fig. 3) was applied on the beam and it was increased monotonically until failure. Load and vertical displacement ($s_a$ in Fig. 3) were monitored by the linear variable differential transducer within the testing machine.

Using the quantities defined in Fig. 3, it is possible to experimentally determine moment on the connection $M = LP$ and the connection rotation $\theta = \theta_{cd} - \theta_{ce}$. Furthermore, $\theta_{cd} = \frac{s_1 - s_2}{k_{12}}$ is the total rotation of the connector and $\theta_{ce} = \frac{Mh_c}{16EJ_c}$ is the elastic rotation of the column at the level of the intersection with the beam; with: $h_c$ the height of the column, $E$ the elastic modulus of steel, $J_c$ the inertia moment of the column, $s_1$ and $s_2$ the horizontal displacements measured by wire-actuated

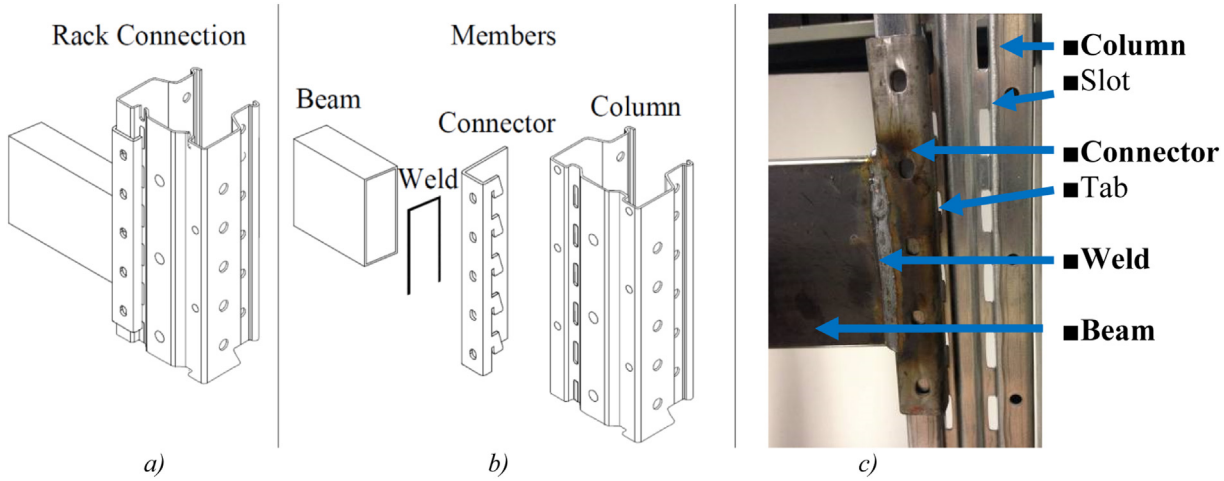


**Fig. 1.** a) Rack connection 3D view; b) Members of rack connection; c) Front view of rack connection and its members identified.

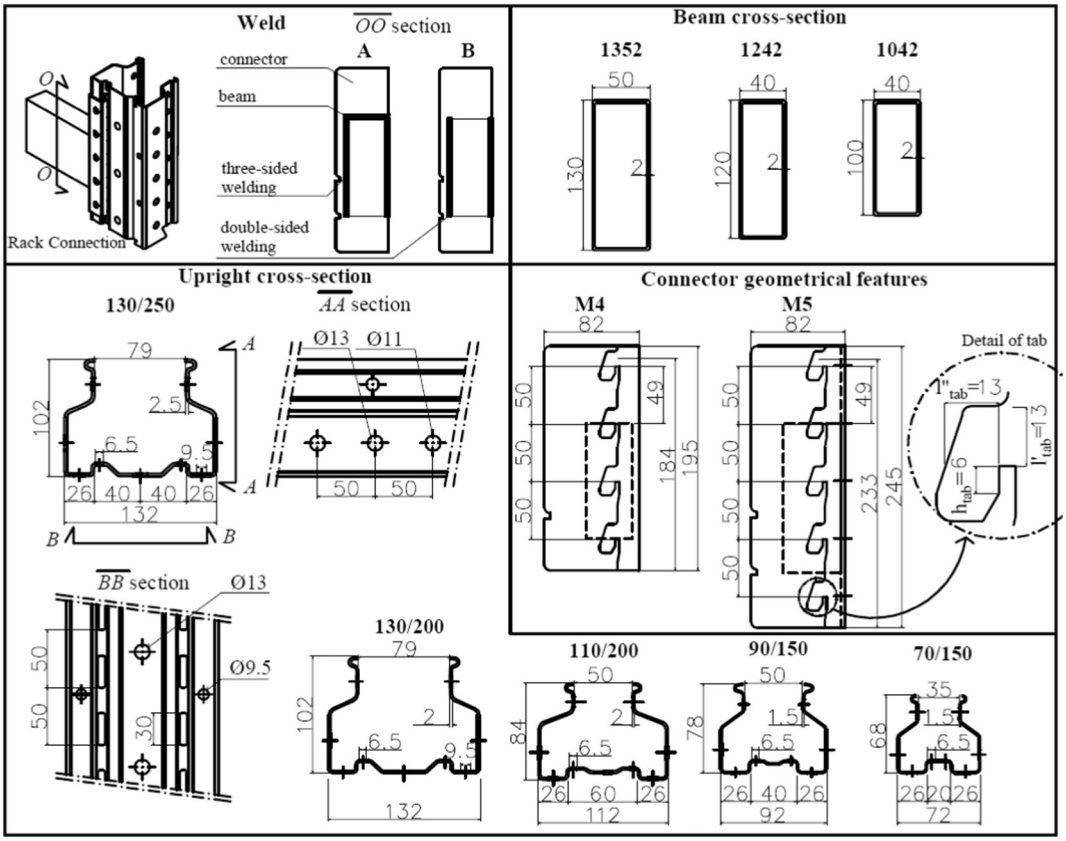


**Fig. 2.** Geometrical features of rack connection members.

encoders placed on top and bottom of the beam-end section, and $k_{12}$ is their relative distance (Fig. 3). Testing procedures, instrumentations and detailed test results of analysed joints can be found in [16].

### 2.3. Mechanical model

To analytically evaluate the initial rotational stiffness and flexural capacity of rack connections, a mechanical model based on the Component Method (CM) was developed and validated in [21,22]. The CM can be applied to any kind of connection provided that the basic sources of strength and deformation are properly identified and modelled [29]. The CM can be organized in three phases. The first is to identify the components in the connection, contributing to structural response. In the second phase each component is modelled via a force-displacement relationship. Bilinear elasto-plastic models (defined by an initial stiffness and an ultimate strength) are used for components that contribute to the stiffness and strength of the connection, whereas a rigid plastic model is used for components that effect connection strength, but not stiffness. These component models are introduced into the mechanical model of the overall connection with springs joined in series or parallel, each with their own lever arm and axial stiffness [30]. In the last phase,

**Table 2**
Rack connections tested and members used to assemble them (● Experimental Test, ■ Numerical Test).

| Beam | Weld | Connector | Column | | | | |
|---|---|---|---|---|---|---|---|
| | | | 70/150 | 90/150 | 110/200 | 130/200 | 130/250 |
| 1042 | A | M4 | ● - ■ | ● - ■ | ■ | ■ | ■ |
| 1242 | A | M5 | ● - ■ | ● - ■ | ● - ■ | ● - ■ | ■ |
| 1352 | A | M5 | ■ | ● - ■ | ● - ■ | ● - ■ | ● - ■ |
| 1042 | B | M4 | ■ | ■ | ■ | ■ | ■ |
| 1242 | B | M5 | ■ | ■ | ■ | ■ | ■ |
| 1352 | B | M5 | ■ | ■ | ■ | ■ | ● - ■ |

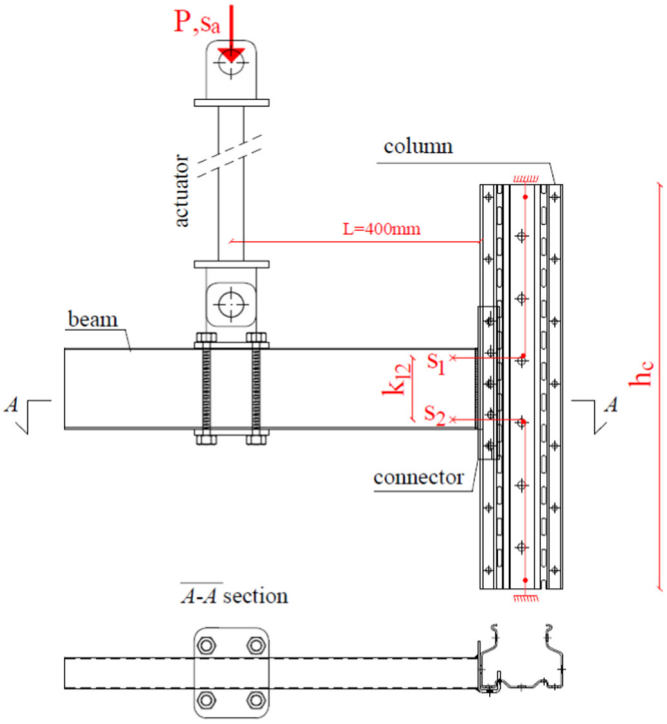


**Fig. 3.** Instrumentation of the experimental tests.

**Table 3**
Ultimate flexural strength and initial stiffness of contributing rack connection components.

| Member | Component | | Model | Ultimate Strength | Initial Stiffness |
|---|---|---|---|---|---|
| Weld | a | Weld | rigid-plastic | $F_{wel}\frac{J_w f_{y,w}}{h_b y_w}$ | ∞ |
| Beam | b | Beam flange tension zone | rigid-plastic | $F_{bf,\,t} = b_{eff,\,b} t_b f_{y,\,b}$ | ∞ |
| | b | Beam flange compression zone | rigid-plastic | $F_{bf,\,c} = b_{eff,\,b} t_b f_{y,\,b}$ | ∞ |
| | c | Connector web tension zone | elasto-plastic | $F_{cow,\,t} = \omega_{co} b_{eff,\,co} t_{co} f_{y,\,co}$ | $k_{cow,t} = \frac{E b'_{eff,co} t_{co}}{d_{wco}}$ |
| | c | Connector web compression zone | elasto-plastic | $F_{cow,\,c} = \omega_{co} b_{eff,\,co} t_{co} f_{y,\,co}$ | $k_{cow,c} = \frac{E b'_{eff,co} t_{co}}{d_{wco}}$ |
| Connector | d | Connector in bending tension zone | elasto-plastic | $M_{co,\,b} = W_{pl,\,co} f_{y,\,co}$ | $k = \frac{1}{\frac{l_1^3}{3EJ_{co}} + \frac{1}{EJ_{co}}(\frac{l_2^2 l_1}{2} - \frac{l_2^3}{2} + \frac{l_2^3}{3}) + \frac{1.2 l_1}{GA_{co}} + \frac{1.2 l_2}{GA_{co}}}$ |
| | d | Connector in bending compression zone | elasto-plastic | $M_{co,\,b} = W_{pl,\,co} f_{y,\,co}$ | $k = \frac{1}{\frac{(2z_c)^3}{8EJ_{co}} + \frac{1.2(z_c)}{GA_{co}}}$ |
| | e | Tabs in bending and in shear | elasto-plastic | $F_{t,s} = \frac{f_{u,co} A_{v,tab}}{\sqrt{3}}$ | $k_{t,s} = \frac{1}{(\frac{l_F^3}{3EI} + \frac{1.2 l_F}{GA_v})}$ |
| | f | Column web in punching | elasto-plastic | $F_{cw,\,p} = 0.6 d_m t_{cw} f_{u,\,cw}$ | $k_{cw,p} = \frac{1}{(\frac{\chi l_{cw,p}}{4GA_{cw,p}} + \frac{l_{cw,p}^3}{192EJ_{cw,p}})}$ |
| | g | Column web bearing | elasto-plastic | $F_{cw,\,b} = 2.5\alpha f_{u,\,cw} h_{tab} t_{cw}$ | $k_{cw,\,b} = 12 k_b k_t h_{tab} f_{u,\,cw}$ |
| | h | Column web in tension | elasto-plastic | $F_{cw,\,t} = \omega b_{eff,\,t} t_{cw} f_{y,\,cw}$ | $k_{cw,t} = \frac{E b'_{eff,t} t_{cw}}{d_{wc,t}}$ |
| | h | Column web in compression | elasto-plastic | $\min: F_{cw,b} = F_{cw,cr}[\frac{1}{\lambda}(1-\frac{0.22}{\lambda})]\ F_{cw,\,cr} = \omega b_{eff,\,c} t_{cw} f_{y,\,cw}$ | $k_{cw,c} = \frac{E b'_{eff,c} t_{cw}}{d_{wc,c}}$ |
| Column | i | Column web in shear | elasto-plastic | $F_{cw,s} = \frac{f_{y,cw} A_{vc,net}}{\sqrt{3}}$ | $k_{cw,s} = \frac{0,38E}{(\frac{\sum h_1}{A_{vc}} + \frac{\sum h_2}{A_{vc,net}})}$ |

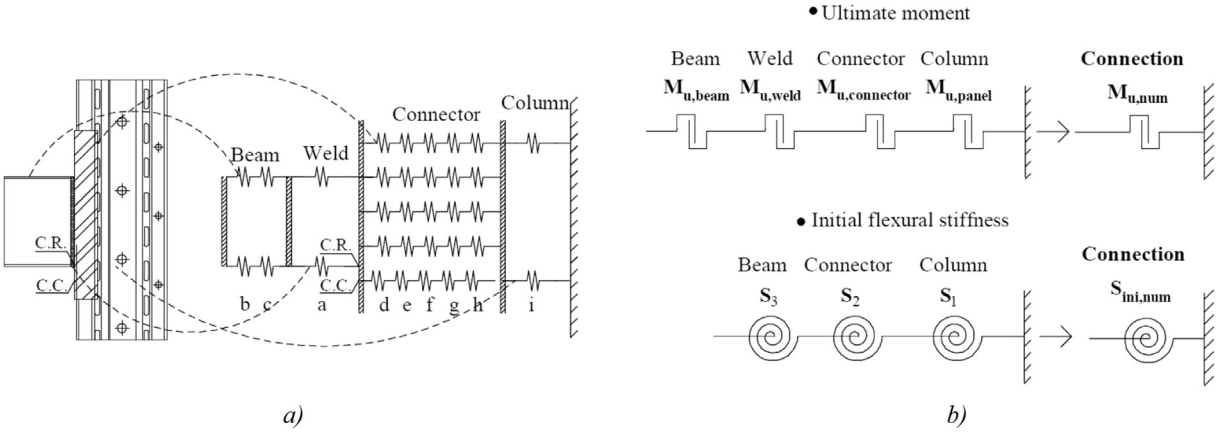


**Fig. 4.** a) Mechanical model to predict the connection capacity ($M_{u,num}$) and the initial stiffness($S_{ini,num}$). b) Members influencing connection ultimate strength and stiffness.

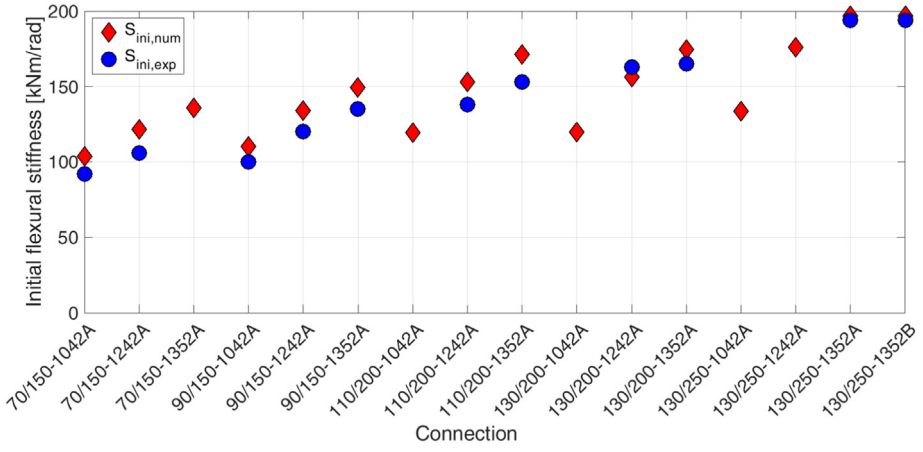


**Fig. 5.** Numerical initial rotational (flexural) stiffness $S_{ini,num}$ and experimental initial rotational stiffness $S_{ini,exp}$.

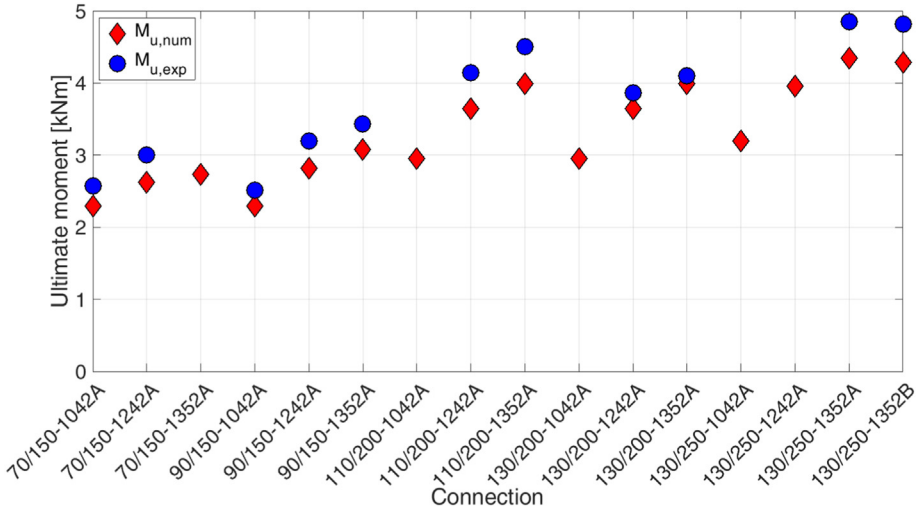


**Fig. 6.** Numerical ultimate flexural strength (moment) $M_{u,num}$ and experimental ultimate moment $M_{u,exp.}$

flexural strength (ultimate moment $M_{u,num}$) and initial elastic rotational stiffness ($S_{ini,num}$) of the joint are predicted. The relationships for the initial stiffness and an ultimate strength implemented in the CM are reported in Table 3. In the CM, components are assumed to have infinite ductility; thus the rotational capacity of the connection cannot be predicted.

The mechanical model is established based on a set of realistic assumptions, taking advantage of the Eurocode 3 framework for determining the theoretical load-displacement behaviour of basic components [30], as well as the theoretical model of boltless connections presented in [31]. A detailed description of the identified rack connection component models can be found in [21]. It is worth noting here that force transfer in rack connections differs in the tension and compression zones. In the tension zone, forces are transferred through tabs while in compression zone, force is transferred through contact between the connector bottom flange and the column.

A sketch of the mechanical model of a rack connection with an M5 connector (five tabs, as shown in Table 2) is shown in Fig. 4 a) as an example. Springs representing the behaviour of the components of the weld (weld type *a*, as shown in Table 3) and of the beam (*b*, *c*) are located at the level of the beam flanges. The springs representing the connector components (*d, e, f, g, h*) are located at the level of tabs in tension zone, and at the centre of compression in compression (denoted CC in Fig. 4 a) zone. The lever arm of the spring representing the column web in shear (*i*) is equal to the distance from the centre of compression and the point of the application of the reaction force in tension zone. The centre of rotation (denoted CR in Fig. 4 a) is assumed at the level of beam bottom flange. The ultimate behaviour of connection is described assuming the plastic distribution of internal forces and the weakest component governs the resistance of each member. The moment capacity of the connection $M_{u,num}$ can be evaluated by: $M_{u,\ num} = \min(M_{u,\ weld}; M_{u,\ beam}; M_{u,\ connector}; M_{u,\ panel})$ where: $M_{u,weld}$ is the ultimate bending moment of the weld, $M_{u,beam}$ is the ultimate bending moment of the beam, $M_{u,connector}$ is the ultimate bending moment of the connector and $M_{u,panel}$ is the ultimate bending moment of the column panel (Fig. 4 b).

The mechanical model used to predict the initial rotational stiffness is shown in Fig. 4 a). In accordance with [30] axial springs are transformed into rotational springs: $S_1$ for the column panel, $S_2$ for the connector and $S_3$ for the beam. The prediction of the initial rotational stiffness $S_{ini,num}$ of the entire connection is then obtained from $S_{ini,num} = \frac{1}{\sum_{n=1}^{3}\frac{1}{S_n}}$ (Fig. 4 b). As a consequence of assuming rigid plastic behaviour for the weld component (*a*), it does not influence flexural stiffness of the connection.

### 2.4. Experimental results

The experimental and numerical initial rotational stiffnesses, $S_{ini,exp}$ and $S_{ini,num}$, respectively, are shown in Fig. 5 while the experimental and numerical ultimate flexural strengths, $M_{u,exp}$ and $M_{u,num}$, respectively, are shown in Fig. 6.

The differences between the numerical and experimental results for initial rotational stiffness ($(S_{ini,num}\text{-}S_{ini,exp})/S_{ini,exp}$ *[%]*) and flexural

**Table 4**
Difference between experimental and numerical initial rotational stiffness and ultimate flexural strength of tested rack connections ($(S_{ini,num}\text{-}S_{ini,exp})/S_{ini,exp}$ *[%]* and ($(M_{u,num}\text{-}M_{u,exp})/M_{u,exp}$ *[%]*) and observed experimental failure mode.

| Connection | Stiffness $\frac{(S_{ini,num}-S_{ini,\ exp})}{S_{ini,\ exp}}$ [%] | Moment $\frac{(M_{u,num}-M_{u,\ exp})}{M_{u,\ exp}}$ [%] | Failure Mode | |
|---|---|---|---|---|
| | | | Member | Component |
| 70/150-1042A | 13 | −11 | Connector | Column web in compression buckling |
| 70/150-1242A | 15 | −13 | Column | Column web in shear |
| 90/150-1042A | 10 | −8 | Connector | Column web in compression buckling |
| 90/150-1242A | 12 | −12 | Connector | Column web in punching |
| 90/150-1352A | 10 | −10 | Connector | Column web in punching |
| 110/200-1242A | 11 | −12 | Connector | Column web in punching |
| 110/200-1352A | 12 | −11 | Connector | Column web in punching |
| 130/200-1242A | −4 | −6 | Connector | Column web in punching |
| 130/200-1352A | 5 | −3 | Connector | Column web in punching |
| 130/250-1352A | 2 | −10 | Connector | Tabs in shear |
| 130/250-1352B | 2 | −9 | Weld | Collapse of weld |

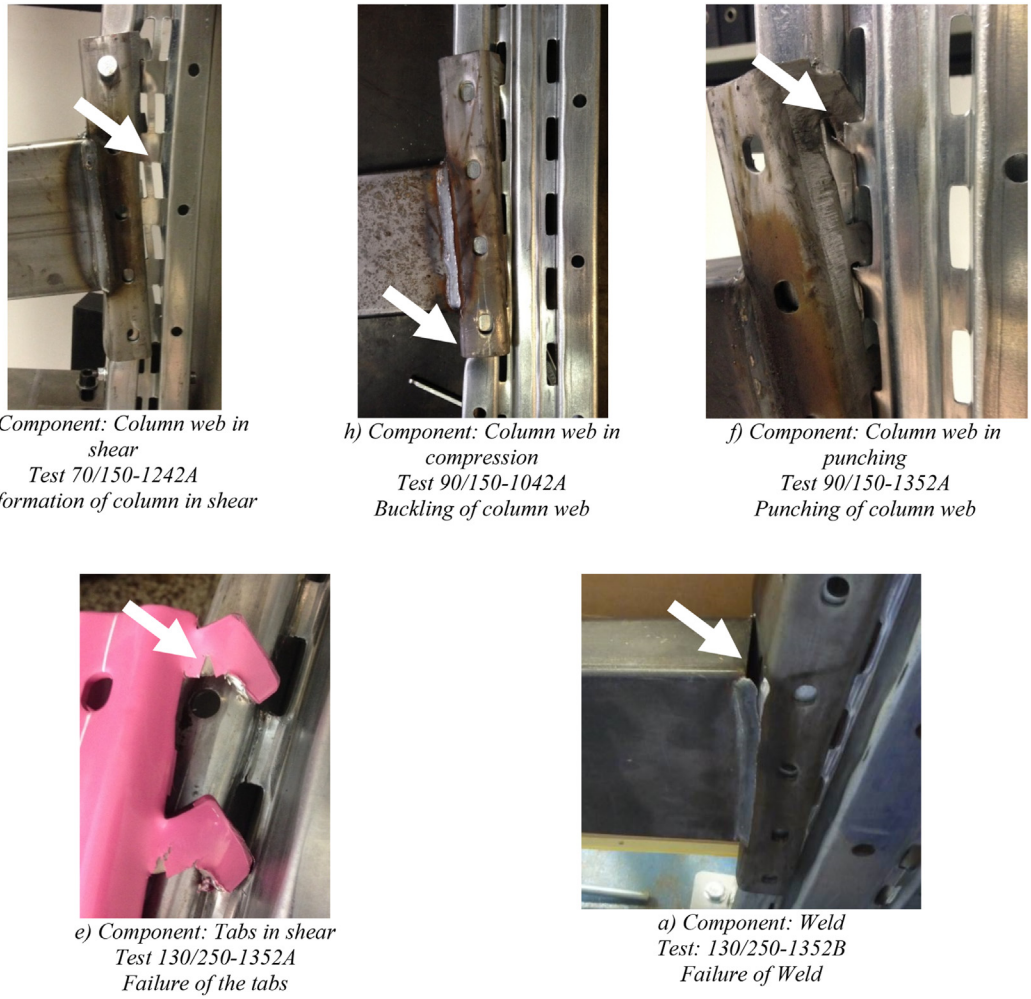


**Fig. 7.** Failure modes observed in experimental tests.

**Table 5**
Design specifications.

| Member | Material | Material Properties - Code | |
|---|---|---|---|
| Beam | S275JRH | EN 10219-1 Cold formed welded structural hollow sections of non-alloy and fine grain steels. Part 1: Technical delivery conditions | [32] |
| Connector | S235JR | EN 10025-2 Hot rolled products of structural steels Part 2: Technical delivery conditions for non-alloy structural steels | [33] |
| Column | S350GD | EN 10346 Continuously hot-dip coated steel flat products Technical delivery conditions | [34] |
| Member | Material | Geometric Features - Code | |
| Beam | S275JRH | EN 10219-2 Cold formed welded structural hollow sections of non-alloy and fine grain steels Part 2: Tolerances, dimensions and sectional properties | [35] |
| Connector | S235JR | EN 10051 Continuously hot-rolled strip and plate/sheet cut from wide strip of non-alloy and alloy steels – Tolerances on dimensions and shape | [36] |
| Column | S350GD | EN 10143 Continuously hot-dip coated steel sheet and strip – Tolerances on dimension and shape | [37] |

**Table 6**
Mechanical requirements.

| Designation | Nominal steel grade | Yield strength $f_y$ [Mpa] | Tensile strength $f_u$ [Mpa] |
|---|---|---|---|
| Beam 1042 – 1242 – 1352 | S275JRH | $275 \le f_y$ | $430 \le f_u \le 580$ |
| Connector M4 – M5 | S235JR | $235 \le f_y$ | $360 \le f_u \le 510$ |
| Column 70/150 – 90/150] | S350GD | $350 \le f_y$ | $420 \le f_u$ |
| Column 110/200 – 130/200] | S350GD | $350 \le f_y$ | $420 \le f_u$ |
| Column 130/250 | S350GD | $350 \le f_y$ | $420 \le f_u$ |

**Table 7**
Geometric tolerances.

| Designation | Tolerance Cross-section [%] | Nominal thickness [mm] | Tolerance thickness [mm] |
|---|---|---|---|
| Beam 1042 (100 × 40 × 2) | ±0.8% | 2 | ±0.2 |
| Beam 1242 (120 × 40 × 2) | ±0.8% | 2 | ±0.2 |
| Beam 1352 (130 × 50 × 2) | ±0.8% | 2 | ±0.2 |
| Connector M4 – M5 Deterministic | | 3.5 | ±0.26 |
| Column 70/150 – 90/150 | | 1.5 | ±0.08 |
| Column 110/200 – 130/200 Deterministic | | 2 | ±0.09 |
| Column 130/250 | | 2.5 | ±0.12 |

**Table 8**
Values of yielding and ultimate stress [N/mm$^2$] of rack connection member steel.

| Values | Beam | | Connector | | Column | | | | | |
|---|---|---|---|---|---|---|---|---|---|---|
| Nominal Thickness [mm] | $t_b = 2$ | | $t_{co} = 3.5$ | | $t_{cw} = 1.5$ | | $t_{cw} = 2$ | | $t_{cw} = 2.5$ | |
| Mechanical Properties [N/mm$^2$] | $f_{yb}$ | $f_{ub}$ | $f_{yco}$ | $f_{uco}$ | $f_{ycw}$ | $f_{ucw}$ | $f_{ycw}$ | $f_{ucw}$ | $f_{ycw}$ | $f_{ucw}$ |
| Probabilistic Values | | | | | | | | | | |
| $\mu_{MC}$ | 451 | 471 | 278 | 374 | 406 | 454 | 419 | 480 | 425 | 469 |
| $V_{MC}$ | 0.10 | 0.05 | 0.05 | 0.05 | 0.05 | 0.05 | 0.05 | 0.05 | 0.11 | 0.08 |
| Probability Distribution | Normal | Normal | Normal | Normal | Normal | Normal | Normal | Normal | Normal | Normal |
| Experimental Values | | | | | | | | | | |
| $\mu_{exp}$ [N/mm$^2$] | 451 | 471 | 278 | 374 | 406 | 454 | 419 | 480 | 425 | 469 |
| $V_{exp}$ | 0.10 | 0.01 | 0.05 | 0.05 | 0.03 | 0.03 | 0.04 | 0.05 | 0.11 | 0.08 |
| Deterministic Values | | | | | | | | | | |
| $f_{Det}$ [N/mm$^2$] | 451 | 474 | 282 | 366 | 416 | 461 | 416 | 460 | 416 | 461 |

**Table 9**
Ranges of geometric parameters.

| Designation | Range cross-section H = height - B = base [mm] | Nominal thickness t [mm] | Range thickness [mm] |
|---|---|---|---|
| Beam 1042 (100 × 40 × 2) | H [99.2–100.8] – B [39.68–40.32] | 2 | [1.9–2.1] |
| Beam 1242 (120 × 40 × 2) | H [119.04–120.96] – B [39.68–40.32] | 2 | [1.9–2.1] |
| Beam 1352 (130 × 50 × 2) | H [128.96–131.04] – B [49.6–50.4] | 2 | [1.9–2.1] |
| Connector M4 – M5 Deterministic | | 3.5 | [3.24–3.76] |
| Column 70/150 – 90/150 | | 1.5 | [1.42 - 1.58] |
| Column 110/200 – 130/200 Deterministic | | 2 | [1.91 - 2.09] |
| Column 130/250 | | 2.5 | [2.38–2.62] |

**Table 10**
Differences ($M_{MC}$-$M_{Det}$)/$M_{Det}$ [%] in the evaluation of the ultimate moment. (MC) Monte Carlo simulations, (Det) Deterministic values.

| Beam | Weld | Connector | Column | | | | |
|---|---|---|---|---|---|---|---|
| | | | 70/150 | 90/150 | 110/200 | 130/200 | 130/250 |
| 1042 | A | M4 | −1.75% | −1.49% | 2.16% | 2.16% | −0.21% |
| 1242 | A | M5 | −2.80% | −1.49% | 1.99% | 1.99% | −0.82% |
| 1352 | A | M5 | −2.43% | −1.50% | 2.72% | 2.72% | 1.22% |

resistance ($(M_{u,num}- M_{u,exp})/ M_{u,exp}$ [%]) are reported in Table 4, with observed failure modes from the experimental tests (Fig. 7).

Generally, the mechanical model slightly overestimates stiffness (Fig. 5) and underestimates moment (Fig. 6) but results agree. Examining connections with identical columns, increasing the beam cross-section and the number of tabs in the connector generally increase stiffness and moment (Fig. 5 and Fig. 6). In connections with the same beam and connector, increasing the column cross-section increases stiffness (Fig. 5), while moment is dependent on failure mode (Fig. 6).

As the welded connection does not influence deformation at the joint, it has no impact on initial rotational stiffness. Two-sided welds (as in test 130/250-1352B) do indeed reduce connection flexural capacity compared to three sided welds (test 130/250-1352A).

## 3. Probabilistic model

Allowable tolerances on geometric properties and material properties for rack connection members as defined by current design specifications are shown in Table 5. Mechanical and geometric requirements for each rack connection member are summarized in.

Table 6 and Table 7 respectively.

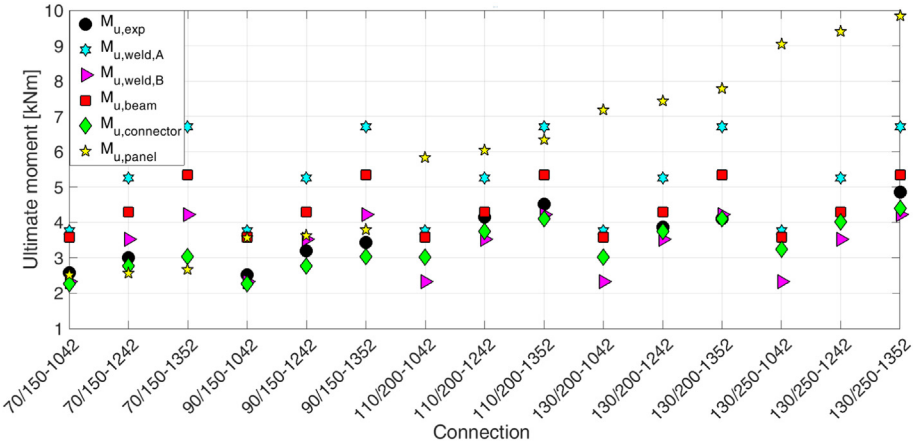


**Fig. 8.** Mean ultimate moments for each rack connection member (weld: $M_{u,weld,A}$ $M_{u,weld,B;}$ beam: $M_{u,beam;}$ connector: $M_{u,connector;}$ column: $M_{u,panel}$) obtained from Monte Carlo simulation and experimental ultimate moment ($M_{u,exp}$).

**Table 11**
Connection members and their component with highest collapse probability.

| Connection | Failure Mode | |
|---|---|---|
| | Member | Component |
| 70/150-1042A | Connector | Column web in compression Buckling |
| 70/150-1242A | Column | Column web in shear |
| 70/150-1352A | Column | Column web in shear |
| 90/150-1042A | Connector | Column web in compression Buckling |
| 90/150-1242A | Connector | Column web in punching |
| 90/150-1352A | Connector | Column web in punching |
| 110/200-1042A | Connector | Column web in punching |
| 110/200-1242A | Connector | Column web in punching |
| 110/200-1352A | Connector | Column web in punching |
| 130/200-1042A | Connector | Column web in punching |
| 130/200-1242A | Connector | Column web in punching |
| 130/200-1352A | Connector | Column web in punching |
| 130/250-1042A | Connector | Tabs in shear |
| 130/250-1242A | Connector | Tabs in shear |
| 130/250-1352A | Connector | Tabs in shear |
| 70/150-1042B | Connector | Column web in compression Buckling |
| 70/150-1242B | Column | Column web in shear |
| 70/150-1352B | Column | Column web in shear |
| 90/150-1042B | Connector | Column web in compression Buckling |
| 90/150-1242B | Connector | Column web in punching |
| 90/150-1352B | Connector | Column web in punching |
| 110/200-1042B | Weld | Collapse of weld |
| 110/200-1242B | Weld | Collapse of weld |
| 110/200-1352B | Connector | Column web in punching |
| 130/200-1042B | Weld | Collapse of weld |
| 130/200-1242B | Weld | Collapse of weld |
| 130/200-1352B | Connector | Column web in punching |
| 130/250-1042B | Weld | Collapse of weld |
| 130/250-1242B | Weld | Collapse of weld |
| 130/250-1352B | Weld | Collapse of weld |

For beams, which are roll-formed tubular cross-sections, geometric tolerances exist for their shape and thickness. For columns and connectors, which are stamped and folded, tolerances exist only for thickness; due to their irregular and unusual shape, shape tolerances are assumed to be deterministic.

Table 6 and Table 7 serve as initial assumptions for the Monte Carlo simulations performed herein.

### 3.1. Characterization of random variables

The mean ($\mu_{MC}$), coefficient of variation ($V_{MC}$) and probability distribution adopted in Monte Carlo simulations for material properties (yielding stress $f_{yi}$ and ultimate stress $f_{ui}$) of each connection member (beam (subscript b), connector (subscript co), and column (subscript cw)) are reported in Table 8. Properties of material random variables were determined through six available coupon tests performed in accordance with [38] on different steel coils used for each member. The experimental mean stress ($\mu_{exp}$) and the corresponding experimental coefficient of variation ($V_{exp}$) are reported in Table 8. This coefficient of variation was <0.05 for several test sets ($f_{ub}$, $f_{ycw}$ $f_{ucw}$). In the judgment of the authors, these coefficients of variation are not representative of typical variability and it would have been imprudent to adopt such low values in a study of connection uncertainty. Therefore, for those material parameters the coefficient of variation has been set to a minimum value of 0.05.

The deterministic values for material properties ($f_{Det}$) used to obtain the numerical results shown in Section 2.4 can be found in Table 8. Deterministic values $f_{Det}$ were obtained by coupon tests on the coil steel of rack connection members described in Section 2.1. These deterministic values, corresponding to the experimental connection tests, differ only slightly from the mean values of the properties used in the probabilistic analysis.

For Monte Carlo simulations, the Young's modulus E, was assumed normal, with $V_{MC} = 0.1$, the steel shear modulus $G = E/[2(1 + \nu)]$, was chosen as a dependent random variable, with $\nu = 0.3$ the Poisson's ratio. Uniformly distributed pseudorandom values, in the ranges defined by design code tolerances, are adopted for the member geometric parameters (Table 9).

### 3.2. Rack connection flexural resistance probabilistic analysis

To characterize the stochastic response of rack connections, 10,000 samples are conducted on each rack connection assembly in the Monte Carlo simulation (Table 2), with component material property and geometric uncertainty as described in Section 3.1. The difference $(M_{MC}\text{-}M_{Det})/M_{Det}$ between the mean from the simulations ($M_{MC}$) and the deterministic value ($M_{Det}$), for the ultimate moment of connection with a weld type A, are reported in Table 10.

The ratio $(M_{MC}\text{-}M_{Det})/M_{Det} \le 0$ indicates detrimental system effects: the mean of the ultimate moment is lower than the deterministic mean and therefore system effects are not beneficial. Thus, a design that uses mean member properties to predict the flexural capacity of the rack joint will over-estimate the mean connection ultimate moment. In connections where $(M_{MC}\text{-}M_{Det})/M_{Det} \ge 0$, a design using mean member properties will under-estimate the ultimate moment of the rack joint. In these connections, system effects increase flexural capacity. However, it should be noted that in both cases the mean of the ultimate moment obtained by Monte Carlo simulation is very close to deterministic one.

The mechanical model can also provide insight into connection failure mode. Flexural capacity $M_{u,num}$ is the minimum of the ultimate bending moment of each member: the weld ($M_{u,weld,A}$ for connection with a weld type A, three sided welding, or $M_{u,weld,B}$ for connection

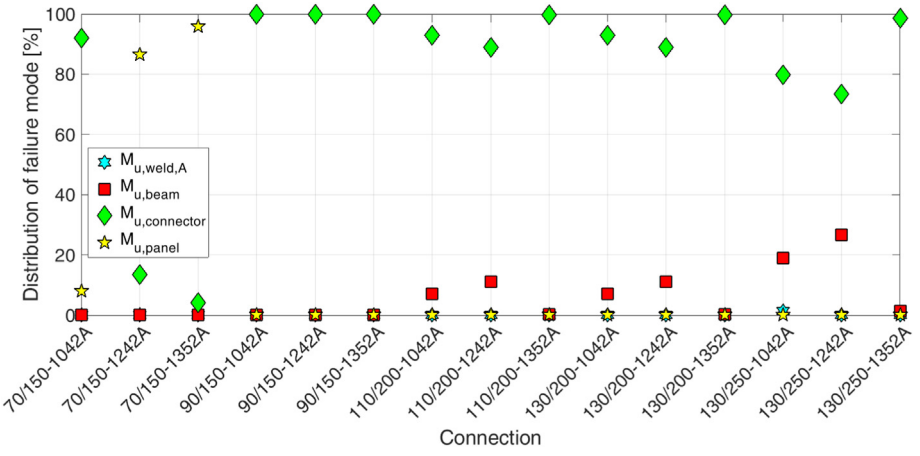


**Fig. 9.** Distribution of failure modes (configurations with weld type A).

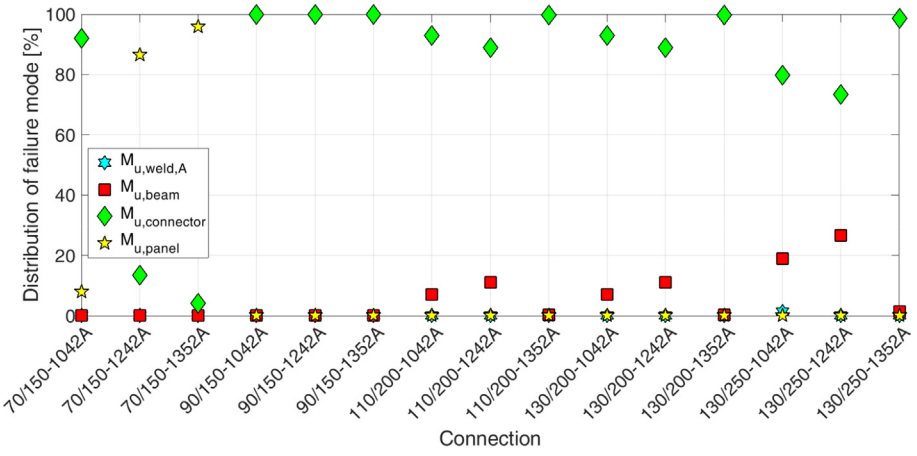


**Fig. 10.** Distribution of failure modes (configurations with weld type B).

**Table 12**
Difference ($(M_{u,numB}\text{-}M_{u,numA})/M_{u,numA}$) [%] in the mean ultimate moment.

| Column | 70 | 70 | 70 | 90 | 90 | 90 | 110 | 110 | 110 | 130 | 130 | 130 | 130 | 130 | 130 |
|---|---|---|---|---|---|---|---|---|---|---|---|---|---|---|---|
| | 150 | 150 | 150 | 150 | 150 | 150 | 200 | 200 | 200 | 200 | 200 | 200 | 250 | 250 | 250 |
| Beam | 1042 | 1242 | 1352 | 1042 | 1242 | 1352 | 1042 | 1242 | 1352 | 1042 | 1242 | 1352 | 1042 | 1242 | 1352 |
| Difference | −2% | 0% | 0% | −2% | 0% | 0% | −23% | −6% | −2% | −23% | −6% | −2% | −27% | −11% | −5% |

**Table 13**
Coefficient of variation for the ultimate moment of members and for the moment capacity of rack joints.

| Column | 70 | 70 | 70 | 90 | 90 | 90 | 110 | 110 | 110 | 130 | 130 | 130 | 130 | 130 | 130 |
|---|---|---|---|---|---|---|---|---|---|---|---|---|---|---|---|
| | 150 | 150 | 150 | 150 | 150 | 150 | 200 | 200 | 200 | 200 | 200 | 200 | 250 | 250 | 250 |
| Beam | 1042 | 1242 | 1352 | 1042 | 1242 | 1352 | 1042 | 1242 | 1352 | 1042 | 1242 | 1352 | 1042 | 1242 | 1352 |
| $M_{u,weld,A}$ | 0.05 | 0.05 | 0.05 | 0.05 | 0.05 | 0.05 | 0.05 | 0.05 | 0.05 | 0.05 | 0.05 | 0.05 | 0.05 | 0.05 | 0.05 |
| $M_{u,weld,B}$ | 0.05 | 0.05 | 0.05 | 0.05 | 0.05 | 0.05 | 0.05 | 0.05 | 0.05 | 0.05 | 0.05 | 0.05 | 0.05 | 0.05 | 0.05 |
| $M_{u,beam}$ | 0.10 | 0.10 | 0.07 | 0.10 | 0.10 | 0.07 | 0.10 | 0.10 | 0.07 | 0.10 | 0.10 | 0.07 | 0.10 | 0.10 | 0.07 |
| $M_{u,connector}$ | 0.05 | 0.05 | 0.05 | 0.05 | 0.05 | 0.06 | 0.05 | 0.05 | 0.05 | 0.05 | 0.05 | 0.05 | 0.06 | 0.06 | 0.06 |
| $M_{u,panel}$ | 0.06 | 0.06 | 0.06 | 0.06 | 0.06 | 0.06 | 0.06 | 0.06 | 0.06 | 0.06 | 0.06 | 0.06 | 0.12 | 0.11 | 0.11 |
| $M_{u,num,A}$ | 0.05 | 0.05 | 0.06 | 0.05 | 0.05 | 0.05 | 0.05 | 0.05 | 0.05 | 0.05 | 0.05 | 0.05 | 0.06 | 0.06 | 0.06 |
| $M_{u,num,B}$ | 0.05 | 0.05 | 0.06 | 0.05 | 0.05 | 0.05 | 0.05 | 0.05 | 0.04 | 0.05 | 0.05 | 0.04 | 0.05 | 0.05 | 0.05 |

with a weld type B, double sided welding, see Fig. 2), the beam $M_{u,beam}$, the connector $M_{u,connector}$ and the column $M_{u,panel}$. The mean of ultimate bending moment of each member as determined from the Monte Carlo simulation is shown in Fig. 8 for all connections along with the experimental ultimate moment $M_{u,exp}$ (Section 1.4).

It can be observed that adopting a weld type B on two sides of the beam-end section, the weld ($M_{u,weld,B}$) is the weakest member and collapses (test: 110/200-1042B, 110/200-1242B, 130/200-1042B, 130/200-1242B, 130/250-1042B, 130/250-1242B and 130/250-1352B). Otherwise (weld type A) the failure mode is related to the weakest component of the connector ($M_{u,connector}$). Regardless of weld type, in tests 70/

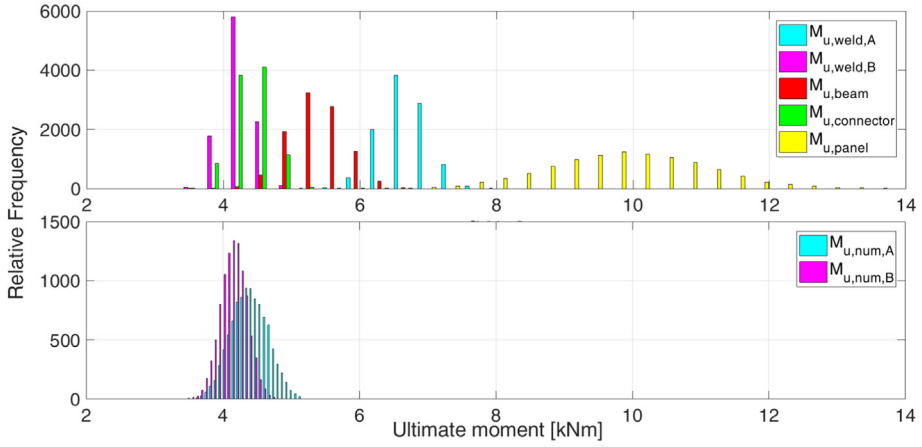


**Fig. 11.** Histograms of member ultimate moment and Histograms of rack connection ultimate moment (weld type A – $M_{u,num,A}$ and weld type B – $M_{u,num,B}$). (Test 130/250–1352).

**Table 14**
Kurtosis ($K.(M_{u,num,i})$) and Skewness ($S.(M_{u,num,i})$) of the ultimate moment distribution for all rack connections (Connection type A, i = A; Connection type B, i = B).

| Column | 70 | 70 | 70 | 90 | 90 | 90 | 110 | 110 | 110 | 130 | 130 | 130 | 130 | 130 | 130 |
|---|---|---|---|---|---|---|---|---|---|---|---|---|---|---|---|
| | 150 | 150 | 150 | 150 | 150 | 150 | 200 | 200 | 200 | 200 | 200 | 200 | 250 | 250 | 250 |
| Beam | 1042 | 1242 | 1352 | 1042 | 1242 | 1352 | 1042 | 1242 | 1352 | 1042 | 1242 | 1352 | 1042 | 1242 | 1352 |
| $K.(M_{u,num,A})$ | 2.85 | 2.93 | 2.93 | 2.92 | 2.92 | 2.92 | 3.35 | 3.55 | 3.04 | 3.35 | 3.55 | 3.04 | 3.16 | 3.36 | 2.73 |
| $K.(M_{u,num,B})$ | 2.97 | 2.93 | 2.93 | 2.95 | 2.92 | 2.92 | 2.96 | 3.27 | 3.04 | 2.96 | 3.27 | 3.04 | 2.96 | 3.16 | 3.01 |
| $S.(M_{u,num,A})$ | 0.01 | −0.08 | −0.03 | 0.09 | 0.09 | 0.08 | −0.07 | −0.15 | 0.07 | −0.07 | −0.15 | 0.07 | −0.16 | −0.21 | 0.03 |
| $S.(M_{u,num,B})$ | −0.07 | −0.08 | −0.03 | −0.05 | 0.09 | 0.08 | 0.00 | −0.19 | −0.09 | 0.00 | −0.19 | −0.09 | 0.00 | −0.12 | −0.04 |

**Table 15**
Differences ($S_{MC}$–$S_{Det}$)/$S_{Det}$ [%] in the evaluation of the initial elastic rotational (flexural) stiffness. (MC) Monte Carlo simulations, (Det) Deterministic values.

| Beam | Weld | Connector | Column | | | | |
|---|---|---|---|---|---|---|---|
| | | | 70/150 | 90/150 | 110/200 | 130/200 | 130/250 |
| 1042 | A | M4 | −0.57% | −0.64% | −0.46% | −0.46% | −0.69% |
| 1242 | A | M5 | −0.61% | −0.70% | −0.06% | −0.04% | −0.46% |
| 1352 | A | M5 | −0.60% | −0.69% | −0.04% | −0.01% | −0.44% |

150–1042, 90/150–1042, 90/150–1242 and 90/150–1352 failure is due to the connector member ($M_{u,connector}$), while in tests 70/150–1242 and 70/150–1352 the failure is due to the collapse of the column panel ($M_{u,panel}$). As expected, in tests with the same column, increasing the geometrical dimensions of the beam (1042 → 1352), $M_{u,weld,A}$, $M_{u,weld,B}$ and $M_{u,beam}$ result in an increase. In increasing the number of tabs in the connector (1042 → 1352), $M_{u,connector}$ increases. Increasing the geometrical dimensions of the column (70/150 → 130/250), the mean ultimate moment of the column panel ($M_{u,panel}$) increases. Weld ultimate moment ($M_{u,weld,B}$ and $M_{u,weld,A}$) and beam ultimate moment ($M_{u,beam}$) depend only on the type of beam. The most probable weakest member and corresponding failure mode, which yield the ultimate moment of the connection assembly, are reported in Table 11. These results are in agreement with the experimental results (Table 4).

The discussion above is based on comparing the mean flexural capacities of the members. In any individual MC simulation, however, the failure mode may differ from that predicted by the mean. In order to illustrate the change in failure mode that occurs from the combination of the random variables, the percentage of failure mode for all rack connections is shown in Fig. 9 and Fig. 10, connections with weld type A and type B respectively.

The difference between the mean ultimate moment of connections with weld type B ($M_{u,num,B}$) and the mean ultimate moment of connections with weld type A ($M_{u,num,A}$), is shown in Table 12.

In all cases shown in Fig. 9, weld ultimate moment ($M_{u,weld,A}$) does not contribute to the governing failure mode. Tests with a weak column (70/150-1242A and 70/150-1352A, see Fig. 9) are more likely to fail due to the collapse of the column panel ($M_{u,panel}$). At the same time, test 70/150-1042A is more likely to fail because of the collapse of the connector member, particularly via column buckling (Table 11). In fact, because of a shorter bottom flange of the connector (connector M4), the compression force in test 70/150–1042 is more concentred compared to test 70/150–1242 and 70/150–1352, leading to the buckling of the column web. In the other connections, with an adequate weld on three sides of the beam-end section (connection type A), the connector member ($M_{u,connector}$) dictates failure.

For connections with weld type B (Fig. 10), $M_{u,weld,B}$ is the limiting factor (excepting test 70/150-1242B, 70/150-1352B, 90/150-1242B, 90/150-1352B, 110/200-1352B and 130/200-1352B) and reduces the ultimate moment of joints (Table 12). Another observation is that for weld type B connections, there is substantial uncertainty in which component causes failure of the connection. In practice, this weld type would generally be avoided. In accordance with [30] the fillet welds should be continuous around the corner for a distance of at least twice the leg length of the weld.

The coefficient of variations (CoV) for the ultimate moment of connection members ($M_{u,weld,A}$ $M_{u,weld,B}$ for weld, $M_{u,beam}$ for beam, $M_{u,connector}$ for connector and $M_{u,panel}$ for column) and connections ($M_{u,num,A}$ for connection type A and $M_{u,num,B}$ for connection type B) are shown in Table 13.

It is worth noting a general reduction in the value of the connection ultimate moment CoV; the mean of the member CoVs is greater than that of the joint (≈ 0.05) (Table 13). This reduction in variability is beneficial and is a consequence of the plastic redistribution of forces in rack joint. To illustrate this uncertainty propagation from the members to the connection, histograms of member and connection ultimate moment are shown in Fig. 11 for test 130/250–1352.

For connection type A, the failure mode is the minimum of $M_{u,connector}$ and $M_{u,beam}$ and the connector ultimately dictates failure. The same connection with the weaker weld (type B) has a higher probability of

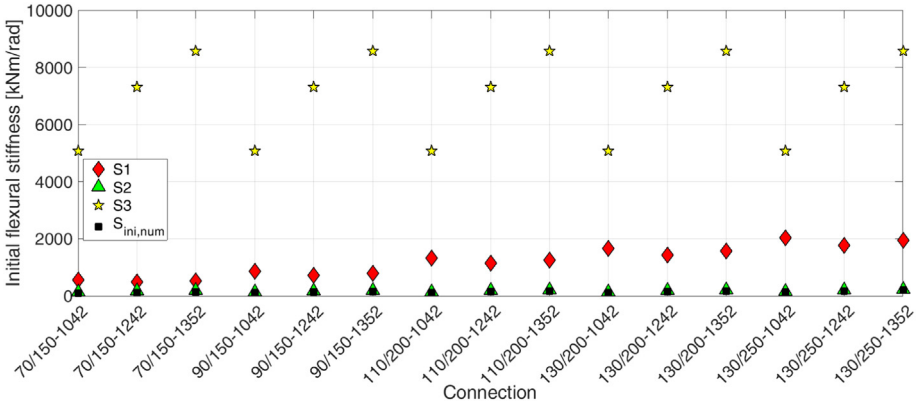


**Fig. 12.** Values of the mean initial elastic rotational (flexural) stiffness for each rack member (column S1, connector S2 and beam S3) and connection ($S_{ini,num}$) obtained in Monte Carlo simulation.

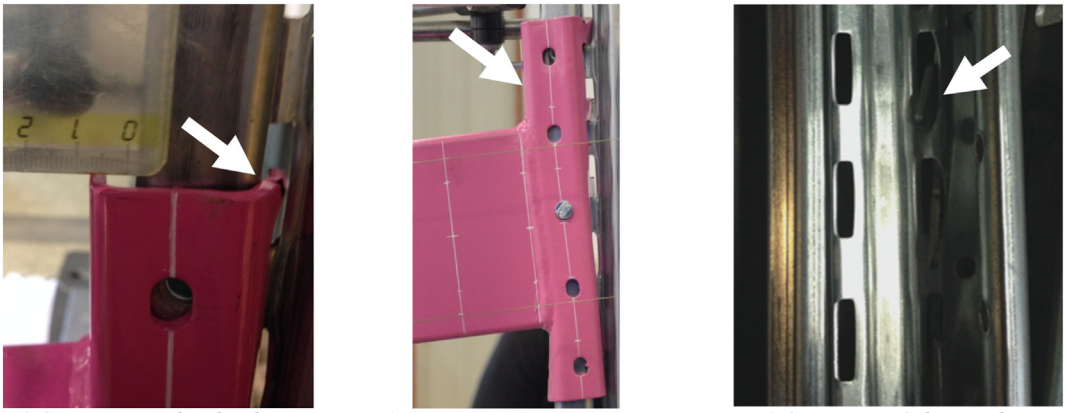

*a) Component: Tab in bending and shear ($K_{t,s}$)*
*Test 130/250-1352A*
*Deformation of tab*

*b) Component: Connector in bending($K_{co,f}$)*
*Test 130/250-1352A*
*Deformation of connector flange*

*c) Component: Column web in bearing($K_{cw,b}$)*
*Test 90/150-T 1242A*
*Deformation of column web at holes*

**Fig. 13.** Connector component deformation observed in experimental tests.

**Table 16**
Coefficient of variation for the flexural stiffness of members and the flexural resistance of rack joints.

| Column | 70 | 70 | 70 | 90 | 90 | 90 | 110 | 110 | 110 | 130 | 130 | 130 | 130 | 130 | 130 |
|---|---|---|---|---|---|---|---|---|---|---|---|---|---|---|---|
| | 150 | 150 | 150 | 150 | 150 | 150 | 200 | 200 | 200 | 200 | 200 | 200 | 250 | 250 | 250 |
| Beam | 1042 | 1242 | 1352 | 1042 | 1242 | 1352 | 1042 | 1242 | 1352 | 1042 | 1242 | 1352 | 1042 | 1242 | 1352 |
| S1 | 0.11 | 0.11 | 0.11 | 0.11 | 0.11 | 0.11 | 0.11 | 0.11 | 0.11 | 0.11 | 0.11 | 0.11 | 0.11 | 0.11 | 0.11 |
| S2 | 0.09 | 0.08 | 0.08 | 0.09 | 0.08 | 0.08 | 0.09 | 0.09 | 0.09 | 0.09 | 0.09 | 0.09 | 0.09 | 0.09 | 0.09 |
| S3 | 0.12 | 0.12 | 0.12 | 0.12 | 0.12 | 0.12 | 0.12 | 0.12 | 0.12 | 0.12 | 0.12 | 0.12 | 0.12 | 0.12 | 0.12 |
| $S_{ini,num}$ | 0.09 | 0.09 | 0.09 | 0.09 | 0.08 | 0.08 | 0.09 | 0.09 | 0.09 | 0.09 | 0.09 | 0.09 | 0.09 | 0.09 | 0.09 |

failure due to the collapse of the weld ($M_{u,weld,B}$) (Fig. 11). The ultimate moment of the connection also decreases ($M_{u,num,B} < M_{u,num,A}$) as well as the CoV of rack joint (see Table 13). To further characterize these rack connections, kurtosis and skewness for the distributions of ultimate moment are shown in Table 14.

A normal distribution with skewness ($\approx 0$) and kurtosis ($\approx 3$) is a good approximation of the connection ultimate moment histogram.

### 3.3. Rack connection rotational stiffness probabilistic analysis

The dimensionless differences ($S_{MC}$-$S_{Det}$)/$S_{Det}$ between the mean (from the simulations - $S_{MC}$) and the deterministic value (based on average properties - $S_{Det}$) of the initial elastic rotational stiffness are reported in Table 15.

($S_{MC}$-$S_{Det}$)/$S_{Det} \leq 0$ for all connections, indicating that the mean stiffness is slightly lower than the deterministic stiffness (minimum value −0.7%) and therefore not all system effects are beneficial. Thus, a design that uses mean member properties to predict the initial rotational stiffness of the rack joint will modestly over-estimate the mean flexural stiffness. The values of the initial rotational stiffness of connection members (column *S1*, connector *S2* and beam *S3*) and rack connection ($S_{ini,num}$) are reported in Fig. 12.

Recall that *S1*, *S2* and *S3* can be considered as three springs in series. The most deformable element is connector (*S2*) whose stiffness is

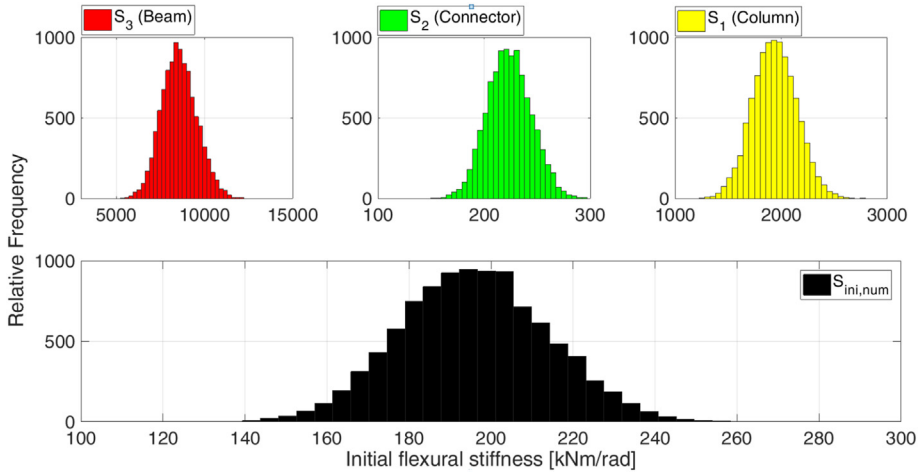


**Fig. 14.** Histograms of flexural stiffness for members and connection (Test 130/250–1352).

**Table 17**
Kurtosis (K.($S_{ini,num}$)) and skewness (S.($S_{ini,num}$)) of flexural stiffness for all rack connections.

| Column | 70 | 70 | 70 | 90 | 90 | 90 | 110 | 110 | 110 | 130 | 130 | 130 | 130 | 130 | 130 |
|---|---|---|---|---|---|---|---|---|---|---|---|---|---|---|---|
| | 150 | 150 | 150 | 150 | 150 | 150 | 200 | 200 | 200 | 200 | 200 | 200 | 250 | 250 | 250 |
| Beam | 1042 | 1242 | 1352 | 1042 | 1242 | 1352 | 1042 | 1242 | 1352 | 1042 | 1242 | 1352 | 1042 | 1242 | 1352 |
| K.($S_{ini,num}$) | 2.83 | 2.85 | 2.85 | 2.81 | 2.83 | 2.84 | 2.84 | 2.85 | 2.87 | 2.84 | 2.84 | 2.86 | 2.90 | 2.90 | 2.90 |
| S.($S_{ini,num}$) | 0.03 | 0.00 | 0.00 | 0.03 | 0.00 | 0.00 | 0.03 | 0.01 | 0.01 | 0.02 | 0.01 | 0.01 | 0.08 | 0.08 | 0.08 |

similar to that of the entire connection ($S_{ini,num}$). The effect of the stiffness of the beam (*S3*) on the connection can be neglected (as neglecting the contribution of beam deformation does not meaningfully change the connection stiffness). As expected, in reducing the cross-section of the column (130/250 → 70/150), the flexural stiffness of the column (*S1*) decreases. Within the connector components, the deformation of the tabs (Fig. 13 a)), connector flange (Fig. 13 b)) and column web in bearing (Fig. 13 c)) have the greatest influence on joint deformation and will govern.

The coefficient of variation (CoV) for the flexural stiffness of connection members (*S1* for column, *S2* for connector and *S3* for beam) and connections ($S_{ini,num}$) are shown in Table 16.

As opposed to the reduction in CoV observed in the ultimate moments of the rack joints, joint flexural stiffness CoV has greater dispersion (≈ 0.09). This effect is a consequence of the connection members acting in series. In determining the ultimate moment of the joint, the weakest component is critical while for stiffness, each component contributes to the overall connection flexural stiffness. The CoV of the overall connection ($S_{ini,num}$) is similar to that of the connector (*S2*) thus confirming the reduced influence of column (*S1*) and beam (*S3*). These results are highlighted by the histograms of the flexural stiffness of members and connection (Fig. 14, for test 130/250–1352).

In Table 17 the values of kurtosis and skewness of the flexural stiffness distributions for all rack connections are reported.

The symmetry of the connection flexural stiffness histograms is highlighted by a skewness ≈ 0 for all connections. A kurtosis mildly <3 allows to assume the normal distribution as a good approximation to fit the connection flexural stiffness histogram.

## 4. Conclusion

The flexural resistance and initial elastic flexural stiffness of CFS rack connection are affected by the local response of connection component. This response derives from the component structural details and it is influenced by the uncertainty in steel mechanical properties and geometrical features. In order to explore the impact of these parameters, Monte Carlo simulation of several rack connection assemblies is developed adopting random values to simulate the effect of the variability in the steel yielding stress, steel ultimate stress and geometrical features of the beam, connector and column. For development of simulations, statistical properties of material random variables were assumed on results of experimental tests, the variability in geometric tolerances was assumed in accordance with current standard code requirements and the structural response of rack joints was modelled by a mechanical model based on the Component Method. Monte Carlo simulations indicate that the variability of geometric and mechanical properties mitigates in the evaluation of the connection ultimate moment (CoV ≈ 0.05). This redistribution occurs due to plasticity in the rack joint and the weakest link fails first. The variability in the flexural stiffness is greater (CoV ≈ 0.09) due to components in series compounding to contribute to total connection stiffness. Finally, a normal probability distribution function well fits for both the connection ultimate moment and initial flexural stiffness histograms.

Results further highlight the effect on failure mode and ultimate moment due to varying connection configurations. A two-sided weld is insufficient. With an adequate weld, connection failure mode mainly depends to the collapse of the weakest component in the connector member. The flexural stiffness of the rack joint is limited by the connector stiffness, and is thus the most critical feature which should be controlled with greater accuracy in the manufacturing process.

## References


[1] G.J. Hancock, Cold-formed steel structures, J. Constr. Steel Res. 59 (4) (2003) 437–487.
[2] K. Peterman, M.J.J. Stehman, R.L. Madsen, S.G. Buonopane, N. Nakata, B.W. Schafer, Experimental seismic response of a full-scale cold-formed steel-framed building. I: System-level response, J. Struct. Eng. 142 (12) (2016), 04016127. .
[3] F.S. Cardoso, K.J.R. Rasmussen, Finite element (FE) modelling of storage rack frames, J. Constr. Steel Res. 126 (2016) 1–14.
[4] N. Baldassino, C. Bernuzzi, Analysis and behaviour of steel storage pallet racks, Thin-Walled Struct. 37 (2000) 277–304.
[5] M. Abdel-Jaber, R.G. Beale, M.H.R. Godley, Numerical study on semi-rigid racking frames under sway, Comput. Struct. 83 (2005) 2463–2475.
[6] C. Bernuzzi, M. Simoncelli, An advanced design procedure for the safe use of steel storage pallet racks in seismic zones, Thin-Walled Struct. 109 (2016) 73–87.
[7] B.W. Schafer, D. Ayhan, J. Leng, P. Liu, D. Padilla-Llano, K.D. Peterman, M. Stehman, S.G. Buonopane, M. Eatherton, R. Madsen, B. Manley, C.D. Moen, N. Nakata, C. Rogers, C. Yu, Seismic response and engineering of cold-formed steel framed buildings, Structure (2016) 197–212.
[8] F.D. Markazi, R.G. Beale, M.H.R. Godley, Experimental analysis of semi-rigid boltless connectors, Thin-Walled Struct. 28 (1997) 57–87.
[9] Dai L., Zhao X. Rasmussen K. J. R. (2018), " Flexural behaviour of steel storage rack beam-to-upright bolted connections. 124 202–217.
[10] AS/NZS 4084, Steel Storage Racking, Standards Australia/ Standards New Zealand, Sydney, Australia, 2012.
[11] RMI. Specifications for the design, testing and utilization of industrial steel storage racks,ANSI MH16.1–2012, Rack Manufactures Institute, Technical report.
[12] EN 15512, Steel static storage systems, European Technical Committee CEN/TC 344, European Specifications, 2009.
[13] C. Bernuzzi, C.A. Castiglioni, Experimental analysis on the cyclic behavior of beam-to-column joints in steel storage pallet racks, Thin-Walled Struct. 39 (2001) 841–859.
[14] Zhao,X., Wang, T., Chen, Y., Sivakumaranc, K. S., (2014), "Flexural behavior of steel storage rack beam to-upright connections", J. Constr. Steel Res. 99 161–175.
[15] P. Prabha, V. Marimuthu, M. Saravanan, S. Arul Jayachandran, Evaluation of connection flexibility in cold formed steel racks, J. Constr. Steel Res. 66 (2010) 863–872.
[16] F. Gusella, G. Lavacchini, M. Orlando, Monotonic and cyclic tests on beam-column joints of industrial pallet racks, J. Constr. Steel Res. 140 (2018) 92–107.
[17] L. Yin, G. Tang, M. Zhang, B. Wang, B. Feng, Monotonic and cyclic response of speed-lock connections with bolts in storage racks, Eng. Struct. 116 (2016) 40–55.
[18] B.P. Gilbert, K.J.R. Rasmussen, Bolted moment connections in drive-in and drive through steel storage racks, J. Constr. Steel Res. 66 (6) (2010) 755–766.
[19] X. Zhao, L. Dai, T. Wanga, K.S. Sivakumaran, Y. Chen, A theoretical model for the rotational stiffness of storage rack beam-to-upright connections, J. Constr. Steel Res. 133 (2017) (269–28).
[20] M.H.R. Godley, Plastic Design of Pallet Rack Beams, Thin-Walled Struct. 29 (1–4) (1997) 175–188.
[21] F. Gusella, M. Orlando, A. Vignoli, K. Thiele, Flexural capacity of steel rack connections via the component method, Open Construct. Build. Technol. J. 12 (2018) 3–16.
[22] F. Gusella, M. Orlando, K. Thiele, Evaluation of rack connection mechanical properties by means of the Component Method, J. Constr. Steel Res. 149 (2018) 207–224.
[23] J. Melcher, Z. Kala, The probabilistic verification of structural stability design procedures, Proceedings of the SSRC 2003 Annual Technical Session Held in Baltimore, MD, SSRC 2003, pp. 557–598.
[24] H. Gervasio, L. Simoes Da Silva, L. Borges, Reliability assessment of the post-limit stiffness and ductility of steel joints, J. Constr. Steel Res. 60 (2004) 635–648.
[25] G. Bian, A. Chatterjee, S.G. Buonopane, S.R. Arwade, C.D. Moen, B.W. Schafer, Reliability of cold-formed steel framed shear walls as impacted by variability in fastener response, Eng. Struct. 142 (2017) 84–97.
[26] B.H. Smith, S.R. Arwade, B.W. Schafer, C.D. Moen, Design component and system reliability in low-rise cold formed steel framed commercial building, Eng. Struct. 127 (2016) 434–446.
[27] M. Orlando, G. Lavacchini, B. Ortolani, P. Spinelli, Experimental capacity of perforated cold-formed steel open sections under compression and bending, Steel Compos. Struct. 24 (2017) 201–211 ISSN:1229-9367.

[28] L. Bertocci, D. Comparini, G. Lavacchini, M. Orlando, L. Salvatori, P. Spinelli, Experimental, numerical, and regulatory P-Mx-My domains for cold-formed perforated steel uprights of pallet-racks, Thin-Walled Struct. 119 (2017) 151–165 (ISSN:0263-8231).
[29] C. Faella, V. Piluso, G. Rizzano, Structural Steel Semi Rigid Connections, Theory, Design and Software, CRC Press, 2000.
[30] Eurocode 3 - Design of Steel Structures- Part. 1-8: Design of Joints. BS EN 1993-1-82005.
[31] L. Ślęczka, A. Kozłowski, Experimental and theoretical investigations of pallet racks connections, Adv. Steel Constr. 3 (2) (2007) 607–627.
[32] EN 10219-1, Cold Formed Welded Structural Hollow Sections of Non-alloy and Fine Grain Steels, 2006.
[33] EN 10025-2, Hot Rolled Products of Structural Steels, 2018.
[34] EN 10346, Continuously Hot-Dip Coated Steel Flat Products, 2018 (Technical delivery conditions).
[35] EN 10219-2, Cold Formed Welded Structural Hollow Sections of Non-alloy and Fine Grain Steels, 2018.
[36] EN 10051, Continuously Hot-Rolled Strip and Plate/Sheet Cut from Wide Strip of Non-alloy and Alloy Steels – Tolerances on Dimensions and Shape, 2018.
[37] EN 10143, Continuously Hot-Dip Coated Steel Sheet and Strip – Tolerances on Dimension and Shape, 2018.
[38] International Standard ISO 6892-1:2009, Metallic materials – Tensile testing Part1: Method of test at room temperature, 2018.